

# Magnetic Quantum Oscillations in $\text{YBa}_2\text{Cu}_3\text{O}_{6.61}$ and $\text{YBa}_2\text{Cu}_3\text{O}_{6.69}$ in Fields of Up to 85 T: Patching the Hole in the Roof of the Superconducting Dome

John Singleton,<sup>1</sup> Clarina de la Cruz,<sup>2,3</sup> R. D. McDonald,<sup>1</sup> Shiliang Li,<sup>4,2</sup> Moaz Altarawneh,<sup>1</sup> Paul Goddard,<sup>5</sup> Isabel Franke,<sup>5</sup> Dwight Rickel,<sup>1</sup> C. H. Mielke,<sup>1</sup> Xin Yao,<sup>6</sup> and Pengcheng Dai<sup>2,3,4</sup>

<sup>1</sup>National High Magnetic Field Laboratory, Los Alamos National Laboratory, MS-E536, Los Alamos, New Mexico 87545, USA

<sup>2</sup>Department of Physics and Astronomy, The University of Tennessee, Knoxville, Tennessee 37996-1200, USA

<sup>3</sup>Neutron Scattering Science Division, Oak Ridge National Laboratory, Oak Ridge, Tennessee 37831, USA

<sup>4</sup>Institute of Physics, Chinese Academy of Sciences, Beijing 100190, China

<sup>5</sup>Clarendon Laboratory, Department of Physics, Oxford University, Oxford, United Kingdom OX1 3PU

<sup>6</sup>Department of Physics, Shanghai Jiao Tong University, Shanghai 200030, China

(Received 12 November 2009; published 25 February 2010)

We measure magnetic quantum oscillations in the underdoped cuprates  $\text{YBa}_2\text{Cu}_3\text{O}_{6+x}$  with  $x = 0.61, 0.69$ , using fields of up to 85 T. The quantum-oscillation frequencies and effective masses obtained suggest that the Fermi energy in the cuprates has a maximum at hole doping  $p \approx 0.11\text{--}0.12$ . On either side, the effective mass may diverge, possibly due to phase transitions associated with the  $T = 0$  limit of the metal-insulator crossover (low- $p$  side), and the postulated topological transition from small to large Fermi surface close to optimal doping (high  $p$  side).

DOI: 10.1103/PhysRevLett.104.086403

PACS numbers: 71.18.+y, 71.45.-d, 74.72.-h

One of the significant landmarks in the study of the “High- $T_c$ ” cuprates is the observation of Shubnikov-de Haas and de Haas-van Alphen oscillations [1–7] in high magnetic fields. Such magnetic quantum oscillations (MQOs) are the signature of a Fermi surface (FS), and their temperature ( $T$ ) and field ( $B$ ) dependence suggest a relatively conventional Fermi liquid [1–5,7,8], rendering some theories of the cuprate normal state untenable [9]. Though there are attempts to explain the MQOs using more exotic models [10–12], these seem unable to describe aspects of the data (e.g., multiple MQO frequencies, MQOs periodic in  $1/B$ , realistic effective masses).

However, published MQOs cover only a restricted region of hole doping  $p$ . In particular, data on underdoped  $\text{YBa}_2\text{Cu}_3\text{O}_{6+x}$  correspond to  $0.49 \leq x \leq 0.54$  ( $0.0925 \leq p \leq 0.10$ ) [1,2,5,7]. As this is also the  $x$  range blighted by the ortho-I/ortho-II structural instability [13], it is natural to ask whether the observed FSs are a consequence of, or related to, this phase separation. Moreover, the only higher- $p$  data for the underdoped side of the superconducting dome are for  $\text{YBa}_2\text{Cu}_4\text{O}_8$  ( $p \approx 0.125\text{--}0.14$  [3,4]). These may be untypical because of the different crystal structure. Here we therefore report MQOs in the underdoped cuprates  $\text{YBa}_2\text{Cu}_3\text{O}_{6.61}$  ( $p \approx 0.11$ ) and  $\text{YBa}_2\text{Cu}_3\text{O}_{6.69}$  ( $p \approx 0.125$ ). We find that both exhibit a dominant MQO frequency  $F \approx 550\text{--}570$  T, similar to the  $\alpha$  frequency observed in the  $0.49 \leq x \leq 0.54$  samples [1,2,5,7,8]. On close examination, the  $p \approx 0.11$  sample exhibits additional MQO frequencies, some attributable to warping of the FS due to a finite interlayer transfer integral. Effective masses  $m^*$  found for both compositions are less than  $2.0m_e$ , lighter than their equivalent in  $\text{YBa}_2\text{Cu}_4\text{O}_8$  [3,4].

Single crystals of  $\text{YBa}_2\text{Cu}_3\text{O}_{6.61}$  and  $\text{YBa}_2\text{Cu}_3\text{O}_{6.69}$  are grown and oxygenated as described before [14]. Samples are polished to sizes  $0.3 \times 0.3 \times 1.5$  mm<sup>3</sup>, with the long axis parallel to  $\mathbf{c}$ . Compositions are inferred by measuring  $T_c$  in a SQUID magnetometer, and using the  $p$  and  $x$  versus  $T_c$  relationships given in Ref. [13]. The MQO experiments employ the same system as in Ref. [4]; a coil of 8–15 turns of 44 or 50-gauge Cu wire is wound around the sample, the planes of the turns roughly perpendicular to  $\mathbf{c}$ . The coil is part of a tank circuit driven by either a tunnel-diode oscillator (TDO) [15] or a proximity-detector circuit (PDC) [16]; shifts in resonant frequency  $f$  are caused by changes in the skin-depth (normal state) or penetration depth (superconducting state) [15]. No significant differences are noted between PDC and TDO data. A heterodyne system measures  $f$ ; the oscillator output is mixed down using two mixer/filter stages to about 1 MHz and the resulting signal digitized directly at  $10^7$  samples/s using a National Instruments PXI-5105 digitizer. Fields are provided by the 85 T Multi-shot (MSM) and 60 T Long-pulse magnets at NHMFL Los Alamos [4,8] and a 65 T short-pulse magnet at Oxford. The purpose of the range of  $dB/dt$  ( $\sim 100\text{--}15\,000$  T s<sup>-1</sup>) is to characterize and eliminate the effects of sample heating due to induced currents and dissipative vortex motion [4]. The field is measured using a pick-up coil calibrated by the belly MQOs of Cu [17]. Four crystals of  $\text{YBa}_2\text{Cu}_3\text{O}_{6.61}$  and two crystals of  $\text{YBa}_2\text{Cu}_3\text{O}_{6.69}$  are studied; results are consistent between crystals of the same  $x$  and between different magnets.

Figure 1 shows data for  $\text{YBa}_2\text{Cu}_3\text{O}_{6.61}$  and  $\text{YBa}_2\text{Cu}_3\text{O}_{6.69}$  measured in the 85 T MSM at  $T = 1.5$  K; samples are heat-sunk to a sapphire chip and immersed in <sup>4</sup>He liquid. Frequencies are obtained by

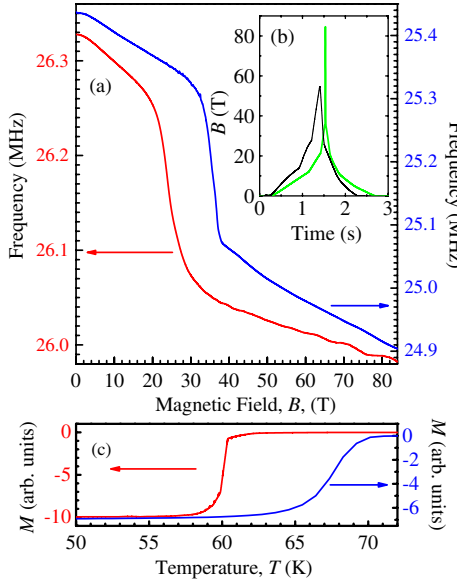


FIG. 1 (color online). (a) PDC frequency  $f$  versus field  $B$  for single crystals of  $\text{YBa}_2\text{Cu}_3\text{O}_{6.69}$  (upper blue trace) and  $\text{YBa}_2\text{Cu}_3\text{O}_{6.61}$  (lower red trace);  $T = 1.5$  K for both. The drop in  $f$  corresponds to the irreversibility field [4,5]. MQOs are visible at high fields for  $\text{YBa}_2\text{Cu}_3\text{O}_{6.61}$ . (b)  $B$  versus time  $t$  profiles for the 60 T Long-pulse and 85 T Multi-shot magnets. (c) SQUID data for the two samples from (a), yielding  $T_c$ .

Fourier transforming the signal using a moving time window 20  $\mu\text{s}$  long, and then adding the offset removed by the mixers. The prominent drop in  $f$  around 25 T ( $x = 0.61$ ) or 35 T ( $x = 0.69$ ) is attributed to the irreversibility field [4,5]. Above this, features are discerned in the data, corresponding to Shubnikov–de Haas oscillations in the conductivity [4,5]. Owing to the proportionality between change in conductivity and shift in  $f$  [15], the conductivity MQOs give oscillations in  $f$ .

We first turn to  $\text{YBa}_2\text{Cu}_3\text{O}_{6.61}$  for which MQOs are visible in the raw data (Fig. 1); below, we see that MQOs are less prominent in  $\text{YBa}_2\text{Cu}_3\text{O}_{6.69}$  due to a shorter apparent scattering time,  $\tau$ . To make the MQOs more visible, the slowly-varying background due to the semiclassical magnetoresistance is removed by subtracting a third-order polynomial in  $B$ . Figure 2(a) shows some resulting MQOs for  $\text{YBa}_2\text{Cu}_3\text{O}_{6.61}$ ; here, random noise from the power supply of the 85 T MSM [8] is mitigated by averaging three upsweeps and three downsweeps and then smoothing using a Savitsky-Golay routine. The resulting data exhibit MQOs above about 40 T. On Fourier-transformation, the dominant peak is at  $F = 570$  T [Fig. 2(b)], similar to the so-called  $\alpha$  MQO frequency (500–550 T) in  $0.49 \leq x \leq 0.54$  samples [1,2,5,8] and the dominant frequency in  $\text{YBa}_2\text{Cu}_4\text{O}_8$  [3,4].

However, in the case of a single extremal FS cross section, one would expect the MQO amplitude to grow uniformly with increasing field [18]. The MQOs in Fig. 2(a) do not do this; they are modulated by what appears to be a beat frequency, a phenomenon noted other

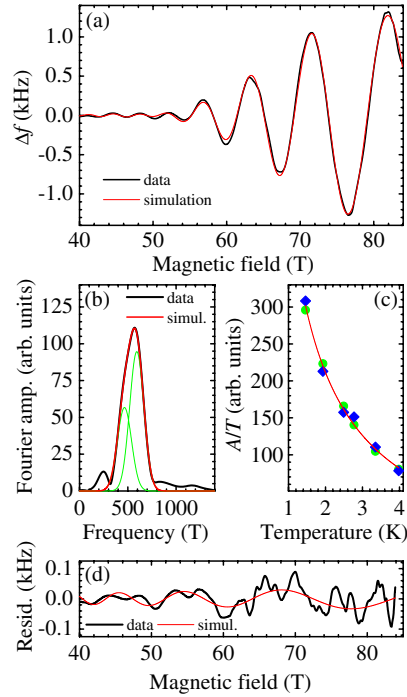


FIG. 2 (color online). (a) PDC resonant frequency  $f$  for a  $\text{YBa}_2\text{Cu}_3\text{O}_{6.61}$  crystal after background subtraction to leave the oscillatory component  $\Delta f$ ; the trace (thick black curve) is an average of three magnet sweeps ( $T = 1.5$  K). The thinner red line is a fit of Eq. (1) for MQO frequencies 589 and 479 T with  $\tau \approx 0.07$  ps. (b) Fourier transform of data in (a) (black thick curve) using a Hann window; the large peak is centered on 570 T. The red curve is a sum of two Gaussians (fine green lines) at 466 and 593 T. (c) Plot of MQO amplitude  $A$  divided by  $T$  versus  $T$ ; diamonds are from the upsweep of  $B$  and dots from the downsweep. The curve is a fit of Eq. (2), giving  $m^* = 1.6 \pm 0.1 m_e$ . (d) Residual [i.e., (data)-(fit)] from (a) versus field (black thicker line). The thinner red curve is a fit of Eq. (1) for a single MQO with  $F = 270 \pm 20$  T.

cuprates [2,4,19]. This is also seen in the Fourier transform [Fig. 2(b)], where the peak at 570 T is obviously asymmetric and may be fitted by two overlapping Gaussians centered on  $466 \pm 10$  and  $593 \pm 5$  T. The presence of two relatively closely spaced Shubnikov–de Haas frequencies with similar amplitudes is suggestive of the beats caused by “neck and belly” oscillations of a quasi-two-dimensional FS that is warped due to a finite interlayer transfer integral  $t_c^\perp$  [2,19]. To model this, we sum two components of the Lifshitz-Kosevich formula [18,19] with MQO frequencies  $F_1$  and  $F_2$ , amplitudes  $a_1$  and  $a_2$ , and phases  $\phi_1$  and  $\phi_2$ :

$$\Delta f = \left( a_1 \cos \left[ \frac{2\pi F_1}{B} + \phi_1 \right] + a_2 \cos \left[ \frac{2\pi F_2}{B} + \phi_2 \right] \right) T B^{-(1/2)} \times \exp \left[ -\frac{\pi m^*}{e\tau B} \right] \left( \sinh \left[ \frac{14.69 m^* T}{B} \right] \right)^{-1}. \quad (1)$$

Here  $m^*$  is the effective mass, and  $\tau^{-1}$  is an effective

scattering rate; we assume that  $m^*$  and  $\tau$  are the same for the neck and belly oscillations. The number 14.69 is valid for  $B$  in Tesla and  $T$  in Kelvin. Independently,  $m^*$  may be constrained by the way in which the amplitude of an individual MQO, or the Fourier amplitude of a transform over a restricted field range varies with  $T$ ;

$$\frac{A}{T} \propto \left( \sinh \left[ \frac{14.69 m^* T}{B} \right] \right)^{-1}, \quad (2)$$

where  $A$  is the amplitude. All of the fits [e.g., Fig. 2(c)] of individual MQOs or Fourier amplitudes yielded  $m^*$  values in the range 1.5–1.7  $m_e$ , irrespective of sample, field range or sweep rate, leading us to  $m^* = 1.6 \pm 0.1 m_e$ . Having constrained  $m^*$ , a fit of Eq. (1) to the data [Fig. 2(a)] yields MQO frequencies  $589 \pm 5$  T and  $479 \pm 5$  T, and  $\tau \approx 0.07$  ps. These values are close to those obtained in the two-Gaussian fit of the transform in Fig. 2(b).

Beside the peak at 570 T in the transform [Fig. 2(b)], there is a feature at  $F \approx 250$  T. This appears to correspond to an actual MQO series, as is seen by subtracting the fitted Eq. (1) in Fig. 2(a) from the data. The residual [Fig. 2(d)] is oscillatory, with a direct fit yielding  $F = 270 \pm 20$  T, close to the value suggested by the peak in the Fourier transform [20]. Unfortunately, the MQOs are too poorly defined to permit estimates of  $m^*$  or  $\tau$ .

To summarize for  $\text{YBa}_2\text{Cu}_3\text{O}_{6.61}$ , our data suggest three FS cross sections, with MQO frequencies 270, 479, and 589 T; other peaks in the transform at higher frequencies [Fig. 2(b)] are attributable to harmonics of these [21]. The 479 and 589 T MQOs are likely the neck and belly oscillations of a warped quasi-two-dimensional FS, with  $m^* = 1.6 \pm 0.1 m_e$ ; this is probably the equivalent of the dominant  $\alpha$  frequency in other underdoped cuprates [1,2,5,8]. The frequency difference,  $\Delta F \approx 110$  T, between neck and belly oscillations suggests [19] an average interlayer transfer integral  $t_c^\perp = \hbar \Delta F / (4m^*) = 2.0 \pm 0.1$  meV for  $\text{YBa}_2\text{Cu}_3\text{O}_{6.61}$ , higher than the values 1.4–1.7 [22] obtained for  $\text{YBa}_2\text{Cu}_3\text{O}_{6+x}$  ( $x = 0.51, 0.54$ ) [2,19]. This increase in  $t_c^\perp$  with  $p$  is not unexpected; the lattice parameter  $c$  declines with  $p$  [13].

Figure 3(a) shows an example of the MQOs observed in  $\text{YBa}_2\text{Cu}_3\text{O}_{6.69}$ . In contrast to  $\text{YBa}_2\text{Cu}_3\text{O}_{6.61}$ , where MQOs

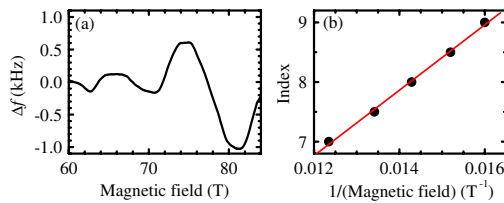


FIG. 3 (color online). (a) PDC resonant frequency for a  $\text{YBa}_2\text{Cu}_3\text{O}_{6.69}$  crystal after background subtraction to leave the oscillatory component  $\Delta f$ ; the trace is a smoothed average of three magnet sweeps ( $T = 1.5$  K). (b) Oscillation index versus reciprocal magnetic field for the MQOs in (a) (points); dips in  $\Delta f$  are indexed by integers and peaks by half integers. The straight line is a fit with a gradient of  $550 \pm 20$  T.

appear around 40 T [Fig. 2(a)], the MQOs here are not distinguishable from the background until about 60 T [Fig. 3(a)]. The nonsinusoidal appearance of the MQOs again suggests the presence of more than one frequency, but sadly, the limited field window over which MQOs are seen both precludes a “neck and belly” analysis [Eq. (1), Fig. 2(a)] and limits the resolution of a Fourier transform. Instead, we plot MQO index versus  $1/B$  in Fig. 3(b) to find a mean frequency of  $550 \pm 20$  T [23]. Fitting the MQO amplitudes versus  $T$  for  $\text{YBa}_2\text{Cu}_3\text{O}_{6.69}$  yields  $m^* = 1.8 \pm 0.3 m_e$ , similar to the  $1.6 \pm 0.1 m_e$  for the analogous MQO frequency in the  $\text{YBa}_2\text{Cu}_3\text{O}_{6.61}$  [Fig. 2(c)]. A Dingle analysis [i.e., a plot of  $\log_e(AB^{1/2} \sinh(14.69 m^* T / B))$  versus  $1/B$ ] [18], where  $A$  is the oscillation amplitude] yields  $\tau \approx 0.04$  ps,  $\sim 2$  times smaller than that for  $\text{YBa}_2\text{Cu}_3\text{O}_{6.61}$ . This accounts for the higher fields required to observe MQOs in  $\text{YBa}_2\text{Cu}_3\text{O}_{6.69}$ . Ref. [24] attributes the dominant Landau-level broadening to quasistatic spin disorder also observed in neutron experiments and parameterized by a correlation length  $\xi$  [25–27]. It is notable that  $\xi$  decreases with increasing  $p$  [25–27], and this may account for the shorter  $\tau$  of the  $x = 0.69$  samples.

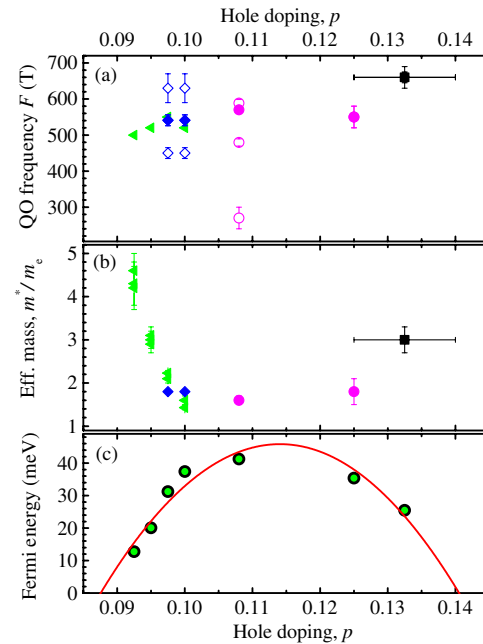


FIG. 4 (color online). (a) Summary of MQO frequencies versus  $p$  for underdoped cuprates: for  $\text{YBa}_2\text{Cu}_3\text{O}_{6+x}$ ,  $\triangleleft$  are from Ref. [8],  $\diamond$  from Ref. [2], and  $\circ$  from this work;  $T_c$  and  $x$  values are converted to  $p$  using Ref. [13].  $\text{YBa}_2\text{Cu}_4\text{O}_8$  data from Refs. [3,4] are squares; the horizontal bar is the spread in  $p$  values given for  $\text{YBa}_2\text{Cu}_4\text{O}_8$  [3,4]. Solid symbols (e.g.,  $\bullet$ ) show the dominant ( $F_\alpha$ ) frequency obtained from Fourier analysis; open symbols are from more detailed analyses [e.g., Figs. 2(a) and 2(d) or Refs. [2,19]]. (b) Effective mass of the dominant ( $\alpha$ ) MQO frequency  $F_\alpha$  versus  $p$ ; symbols are the same as in (a) except  $\diamond$  are from Ref. [7]. (c) Fermi energy from  $F_\alpha$  and  $m^*$ ; for  $p$ s where several values are given, we take the average. Points are data and the curve is a parabolic fit.

Figure 4 compares the data obtained here with similar results from other underdoped cuprates, all of which have a dominant MQO frequency  $F_\alpha \approx 500\text{--}660$  T. Figure 4(a) shows both  $F_\alpha$  and other MQO frequencies  $\leq 1000$  T that have been resolved (this Letter, Refs. [2,19]). If we attribute  $F = 540$  and 450 T for  $p \approx 0.10$  [2] and  $F = 590$  and 480 T for  $p = 0.11$  (this work) to the belly and neck oscillations of the  $\alpha$  Fermi pocket, then there seems to be a trend, smoothly continued by  $\text{YBa}_2\text{Cu}_4\text{O}_8$ , for the  $\alpha$  pocket to grow with rising  $p$  [28]. It also seems that samples from the ortho-I-II region are unexceptional, continuing the trend seen in this work to lower  $p$ . The weaker MQOs with  $F = 630$  T ( $p = 0.975, 0.10$ ) [2]  $F = 270$  T ( $p = 0.11$ ) are qualitatively similar to extra pockets predicted by FS reconstruction due to various types of symmetry breaking; e.g., an incommensurate spin-density wave [29] produces a plethora of FS sheets, both smaller and larger than the  $\alpha$  pocket, while a pocket with  $F \approx 250$  T is an explicit prediction of incommensurate  $d$ -density-wave order [30,31]. Meanwhile, the  $\alpha$  effective masses show a “bowl-shaped” dependence on  $p$ , with a minimum at  $p \approx 0.11$ .

To visualize the effect that these changes have on the carrier system, Fig. 4(c) plots the effective Fermi energy  $E_F$  for the  $\alpha$  pocket,  $E_F = \hbar F_\alpha / m^*$ , using data from Figs. 4(a) and 4(b). It seems that the Fermi energy reaches a maximum at  $p \approx 0.115$ , but decreases either side of this, suggesting that  $m^*$  may diverge at  $p \approx 0.087$  and  $p \approx 0.14$ , the latter  $p$  being poorly constrained by the existing data [32]. The lower  $p$  value suggests the point at which the metal-insulator transition tends to  $T = 0$  [8,33]. The upper may signal the topological transition from small to large FS thought to occur close to optimal doping [4,6], though experimental confirmation of an unreconstructed FS in overdoped  $\text{YBa}_2\text{Cu}_3\text{O}_{6+x}$  is as yet lacking. By analogy with heavy-fermion superconductors [8,34], both of the  $m^*$  divergences may represent quantum-critical phase transitions.

In summary, we report MQO frequencies and effective masses  $m^*$  for the underdoped cuprates  $\text{YBa}_2\text{Cu}_3\text{O}_{6+x}$  with  $x = 0.61, 0.69$ , filling in a considerable gap in the FS versus  $p$  diagram. In conjunction with other data, our results suggest that the Fermi energy reaches a maximum around  $p \approx 0.11\text{--}0.12$ , and collapses on either side due to divergence of  $m^*$ . The divergences are perhaps associated with quantum-critical phase transitions associated with the  $T = 0$  limit of the metal-insulator transition (low- $p$  side), and the topological transition from small to large FS close to optimal doping (high- $p$  side).

This work is supported by the DOE BES grant “Science in 100 T”, DOE DE-FG02-05ER46202, and in part by Division of Scientific User Facilities. NHMFL is funded by DOE, NSF, and the State of Florida. Work at the IOP is supported by the Chinese Academy of Sciences. SJTU is supported by Shanghai Committee of Science and Technology and the MOST of China (2006CB601003). Work at Oxford takes place in the Nicholas Kurti

Magnetic Field Laboratory and is supported by EPSRC. We thank Neil Harrison for useful discussions and John Betts, Mike Gordon, Alan Paris, Daryl Roybal, and Chuck Swenson for extreme technical assistance.

- [1] N. Doiron-Leyraud *et al.*, Nature (London) **447**, 565 (2007).
- [2] A. Audouard *et al.*, Phys. Rev. Lett. **103**, 157003 (2009).
- [3] A. F. Bangura *et al.*, Phys. Rev. Lett. **100**, 047004 (2008).
- [4] E. A. Yelland *et al.*, Phys. Rev. Lett. **100**, 047003 (2008).
- [5] S. E. Sebastian *et al.*, Nature (London) **454**, 200 (2008).
- [6] B. Vignolle *et al.*, Nature (London) **455**, 952 (2008).
- [7] C. Jaudet *et al.*, Phys. Rev. Lett. **100**, 187005 (2008).
- [8] S. E. Sebastian *et al.*, arXiv:0910.2359.
- [9] S. Chakravarty, Science **319**, 735 (2008).
- [10] V. V. Kabanov and A. S. Alexandrov, Phys. Rev. B **77**, 132403 (2008).
- [11] J. A. Wilson, J. Phys. Condens. Matter **21**, 245702 (2009).
- [12] C. M. Varma, Phys. Rev. B **79**, 085110 (2009).
- [13] R. Liang, D. A. Bonn, and W. N. Hardy, Phys. Rev. B **73**, 180505 (2006).
- [14] S. Li *et al.*, Phys. Rev. B **77**, 014523 (2008).
- [15] C. H. Mielke *et al.*, J. Phys. Condens. Matter **13**, 8325 (2001).
- [16] M. M. Altarawneh *et al.*, Rev. Sci. Instrum. **80**, 066104 (2009).
- [17] P. A. Goddard *et al.*, Phys. Rev. B **75**, 094426 (2007).
- [18] D. Shoenberg, *Magnetic Oscillations in Metals* (Cambridge University Press, Cambridge, England, 1984).
- [19] N. Harrison and R. D. McDonald, J. Phys. Condens. Matter **21**, 192201 (2009).
- [20] A similar MQO frequency is seen in magnetic torque measurements of the same samples [S. Cox and R. D. McDonald (unpublished data)].
- [21] In a preliminary account [35] we report a  $F \approx 1990$  T MQO frequency. To date, this is observed in only one sample; the frequency is considered tentative at present.
- [22] The spread in possible values is due to the slightly different fit procedures and  $\Delta F$  values in Refs. [2,19] and the range of effective masses given in the literature.
- [23] The same procedure applied to  $\text{YBa}_2\text{Cu}_3\text{O}_{6.61}$  yields  $580 \pm 10$  T, in agreement with Fourier analysis [Fig. 2(b)].
- [24] N. Harrison, R. D. McDonald, and J. Singleton, Phys. Rev. Lett. **99**, 206406 (2007).
- [25] R. D. McDonald *et al.*, J. Phys. Condens. Matter **21**, 012201 (2009).
- [26] P. Kampf, Phys. Rep. **249**, 219 (1994).
- [27] K. Yamada *et al.*, Phys. Rev. B **57**, 6165 (1998).
- [28] D. LeBoeuf *et al.*, Nature (London) **450**, 533 (2007).
- [29] N. Harrison, Phys. Rev. Lett. **102**, 206405 (2009).
- [30] I. Dimov *et al.*, Phys. Rev. B **78**, 134529 (2008).
- [31] S. Chakravarty and H. -Y. Kee, Proc. Natl. Acad. Sci. U.S.A. **105**, 8835 (2008).
- [32] The conflicting  $p$  values [3,4] for  $\text{YBa}_2\text{Cu}_4\text{O}_8$  are the chief cause of the uncertainty.
- [33] Y. Ando *et al.*, Phys. Rev. Lett. **93**, 267001 (2004).
- [34] P. Monthoux *et al.*, Nature (London) **450**, 1177 (2007).
- [35] J. Singleton *et al.*, Physica (Amsterdam) **404B**, 350 (2009).